Computers in Biology and Medicine 107 (2019) 30–38

Contents lists available at ScienceDirect

Computers in Biology and Medicine

journal homepage: www.elsevier.com/locate/compbiomed

Automated epileptic seizure detection based on break of excitation/inhibition balance

Xiaoya Fan[a,*], Nicolas Gaspard[b], Benjamin Legros[b], Federico Lucchetti[a,c], Rudy Ercek[d], Antoine Nonclercq[a]

[a] Bio, Electro And Mechanical Systems (BEAMS), Université Libre de Bruxelles (ULB), Brussels, Belgium
[b] Department of Neurology, Hôpital Erasme, Université Libre de Bruxelles (ULB), Brussels, Belgium
[c] Laboratoire de Neurophysiologie Sensorielle et Cognitive, Hôpital Brugmann, Brussels, Belgium
[d] Laboratories of Image, Signal processing and Acoustics (LISA), Université Libre de Bruxelles (ULB), Brussels, Belgium

ARTICLE INFO

Keywords:
Epileptic seizure detection
Neural mass model
Parameter identification
Intracranial EEG
Excitation/inhibition balance

ABSTRACT

Physiological models are attractive for seizure detection, as their parameters are related to physiological meanings. We propose an algorithm to early detect epileptic seizures based on automatic estimation of average synaptic gains (excitatory Ae, slow and fast inhibitory B and G) by combining clinical data with a neural mass model. Three indices (Ae/B, Ae/G and Ae/(B + G)), all related to excitation/inhibition balance, were calculated and used as cues to detect seizures. A simple thresholding method was employed. We evaluated the algorithm against the manual scoring of a human expert on intracranial EEG samples from 23 patients suffering from different types of epilepsy. Best performance was achieved using Ae/(B + G) as a cue, i.e. excitation/(slow + fast) inhibition, on temporal lobe epilepsy (TLE) patients. A leave-one-out cross-validation showed that the algorithm achieved 92.98% sensitivity for TLE patients. The median false positive rate was 0.16 per hour, and median detection delay was 14.5 s. Of interest, the threshold values determined by a leave-one-out cross-validation did nearly not vary among TLE patients, suggesting a general excitation/inhibition balance baseline in TLE patients. The same approach could be used with other types of epilepsy by adapting the neural mass model to these types.

1. Introduction

Epilepsy is one of the most common neurological disorders in the world population and affects over 65 million people worldwide [1]. It is characterized by recurrent and unpredictable epileptic seizures [2]. Seizures are caused by sudden, usually brief, temporary electrical disturbance in the brain, which can be seen from the Electroencephalographic (EEG) recordings captured by electrodes placed either directly on the exposed surface of the brain (i.e. intracranial EEG) or along the scalp. The diagnosis of epilepsy often relies on visual inspection of EEG data by an experienced neurophysiologist, which is time-consuming and error-prone, especially in the case of long-term recordings. Moreover, disagreements among neurophysiologists on the same recording are frequent due to the subjective nature of visual analysis and the complexity of EEG waveforms [3]. Automatic seizure detection algorithms could serve as a clinical tool for reviewing EEG data in a more efficient and objective manner and benefit clinical staff by reducing their work load. Moreover, although there are several treatment options, including surgical resection and anti-epileptic drugs, up to 30% of the epileptic patients have no positive response to medication [4]. The unpredictability of seizure occurrence is one of the most disabling aspects of epilepsy and worsens the quality of life of epileptic patients and their families [5]. If seizures could be detected at an early stage (i.e. close to the onset), patients or caregivers could be alerted and potential injuries, even death could be prevented. Alternatively, it could provide an opportunity for on-demand seizure suppression. Together with proper therapy, such as administration of electrical stimulation [6,7], seizures could be stopped earlier or even prevented.

Various EEG-based seizure detection algorithms have previously been proposed. General approach involves extraction and selection of important features, i.e. morphological features [8], spectral features [9], spectra-temporal features [10] such as wavelet-based features [10], which are capable of distinguishing between EEG waveforms recorded from seizure state and non-seizure state. Selected features are then given to classifiers, such as neural networks [11], support vector machines [12,13], fuzzy logic [14,15] or random forests [16,17], which

* Corresponding author. Université libre de Bruxelles, BEAMS CP165/56, Av. F.D. Roosevelt 50, B1050 Bruxelles, Belgium.
E-mail addresses: xiaoya.fan@ulb.ac.be (X. Fan), Nicolas.Gaspard@erasme.ulb.ac.be (N. Gaspard), Benjamin.Legros@erasme.ulb.ac.be (B. Legros), Federico.Lucchetti@ulb.ac.be (F. Lucchetti), rercek@ulb.ac.be (R. Ercek), anoncler@ulb.ac.be (A. Nonclercq).

https://doi.org/10.1016/j.compbiomed.2019.02.005
Received 26 October 2018; Received in revised form 18 January 2019; Accepted 8 February 2019

output the decision of the existence or absence of an epileptic seizure after training. These algorithms have achieved promising results. They could be useful in clinical practice and beneficial for both patients and clinicians. However, the selected features are representations of the EEG waveform rather than neurophysiologically-related. Therefore, they do not reflect the mechanism governing epileptic seizure genesis and can be rather seen as “black boxes".

A model-based approach, on the other hand, can relate the model parameters to neurological mechanisms. Using model parameters as features for seizure detection therefore provides an opportunity to overcome such limitations, allowing this way a more transparent and understandable seizure detection methodology. Besides, advances in our understanding of seizure genesis can be included to enhance neural models and therefore also model-based seizure detection algorithms. Such approaches involve estimating relevant physiological parameters by fitting the models to EEG recordings and hold promise for detecting seizures by analyzing the temporal change of these parameters. Our group has established a methodology to detect seizures automatically at an early stage based on parameter identification of a neural mass model (NMM) from iEEG data and proved the feasibility of such approach [18]. We further implemented a refined version of this NMM and physiologically meaningful key parameters (i.e. average excitatory [Ae], slow [B] and fast [G] inhibitory synaptic gain) were identified. We have found that the excitation/inhibition ratios, i.e. Ae/B, Ae/G and Ae/(B + G), tend to increase around seizure onset and restored before seizure offset [19]. Here, we examined the possibility to translate these findings to implement a model-based automatic seizure detection algorithm. The proposed algorithm was assessed against the manual scoring of an EEG expert, on various patient types, with clinically relevant indicators. The algorithm performance was evaluated in terms of detection strategy, excitation/inhibition ratios used, and compared to the state of the art.

2. Materials and methods

2.1. iEEG database

After approval from the Ethics Committee of Hôpital Erasme, a group of 23 patients with refractory focal epilepsy who underwent intracranial electroencephalography (iEEG) between May 2005 and May 2014 was retrospectively selected from our EEG database. All patients underwent iEEG with 500 Hz sampling frequency and 16-bit resolution. The details of the iEEG data used in this study for each patient are provided in Table 2. In total, 386.83 h of iEEG recordings, containing 91 seizures, were analyzed. Twelve patients (1, 3, 5, 6, 15, 17, 18, 19, 20, 21, 22 and 23) were diagnosed with TLE, with a total recording time of 237.09 h and 60 epileptic seizures. Eight patients (2, 4, 7, 8, 9, 10, 11, and 16) were diagnosed with Frontal Lobe Epilepsy (FLE), with a total recording time of 115.53 h and 23 epileptic seizures. Patients 12, 13, and 14 were respectively diagnosed with Fronto-Temporal Lobe Epilepsy (FTLE), Parieto-Temporal-Occipital Lobe Epilepsy (PTOLE) and Occipital Lobe Epilepsy (OLE), respectively. The total recording time for those patients was 34.21 h and the overall number of epileptic seizures was 8. Patients 9, 11, and 16 were recorded by electrocorticography (ECoG) using subdural grids and strips, while the remaining patients were recorded by stereoelectroencephalography (SEEG). For each recording, one derivation, corresponding to the earliest implicated electrode in the seizure onset zone, has been selected by an expert neurophysiologist. Electrographic onsets of seizures were also marked based on epileptic patterns preceding seizures and were regarded as the ground truth when evaluating the detection algorithm.

2.2. Algorithm overview

The seizure detection algorithm is based on the parameter identification of an NMM. The overview of the algorithm is illustrated in Fig. 1. The signal was first segmented using a 2s-sliding window with 50% overlap. For each window, the key model parameters (i.e. average excitatory synaptic gain Ae, average slow and fast inhibitory synaptic gain B and G) were identified using the algorithm detailed in our previous paper [19,20], which allowed the simulated EEG to best fit the recorded EEG. Afterwards, key model parameters were combined to compute three cues, i.e. Ae/G, Ae/B, and Ae/(B + G), as they were shown to increase during interictal to ictal transition [19]. At last, a decision method was designed to determine whether a seizure has occurred based on the temporal evolution of these cues. These steps are detailed in the following sections.

2.3. EEG modeling and parameter identification

The NMM previously proposed [21] was implemented. It has been validated for generating realistic intracranial epileptiform EEG signals. It mesoscopically models the interactions among the principal cells, excitatory interneuron population, and fast and slow inhibitory interneuron populations. Mathematically, the model is described by 10 first order differential equations [21]. All parameters were set to standard values [22], except the average synaptic gains (i.e. the average excitatory synaptic gain of the principal cells Ae, as well as the average synaptic gains of the slow and fast inhibitory interneuron populations, respectively B and G) that can vary, as previously proposed [22–24]. We employed a window-by-window approach to identify the key parameters by searching the parameter space exhaustively. The iEEG signals were first filtered below 0.16 Hz and above 65 Hz to remove slow baseline drift and electronic noise. Second, a 50 Hz notch filter was used to remove power line noise. After pre-processing, the clinical data was segmented using a 2 s sliding window with a step of 1 s. For each window, the key parameters were identified by minimizing an error function, which was established as the Euclidean distance between the feature vectors estimated from the synthesized and recorded signal, respectively (for more details see Ref. [19]). We made the proposed methodology available in a toolbox[1] integrated in the Statistical Parametric Mapping (SPM) software package,[2] which is widely used in the neuroscience community for the analysis of brain imaging data sequences, such as EEG/MEG, fMRI and PET etc. [25–27]. Although exhaustive search was employed to identify the key model parameters, the computational load was tremendously reduced by pre-calculating the average feature vectors of the simulated data. The computational complexity of the proposed method is linear with the size of the data. The running time for estimating the synaptic gains for 1000 s iEEG data was 180 s when ran on a Windows 7 platform with 2.6 GHz CPU, 4 GB of memory. Therefore, it can be used in a real-time application.

2.4. Seizure detection algorithm

To estimate the occurrence of a seizure, the shift over time of average synaptic gains (excitatory Ae, slow and fast inhibitory B and G) was evaluated. Three cues, Ae/G, Ae/B and Ae/(B + G), were then computed. They are directly related to the balance between excitation and inhibition, which has been reported to play a central role in the transition from background to epileptic activities [19,28,29]. We have shown previously that these cues tend to increase when seizure occurs [19]. Here, we further investigated the feasibility of using any of them for detecting seizure onset. A simple thresholding method was employed: a seizure is detected if one of the cues (Ae/G, Ae/B or Ae/(B + G)) crosses a predefined threshold. It therefore gives a direct interpretation of the break of balance between excitation and inhibition. As a first step, it seemed important to choose such a straightforward and interpretable decision method to give insights into the algorithm

[1] http://beams.ulb.ac.be/research-projects/synaptic-gains-tracking-toolbox.
[2] http://www.fil.ion.ucl.ac.uk/spm/.

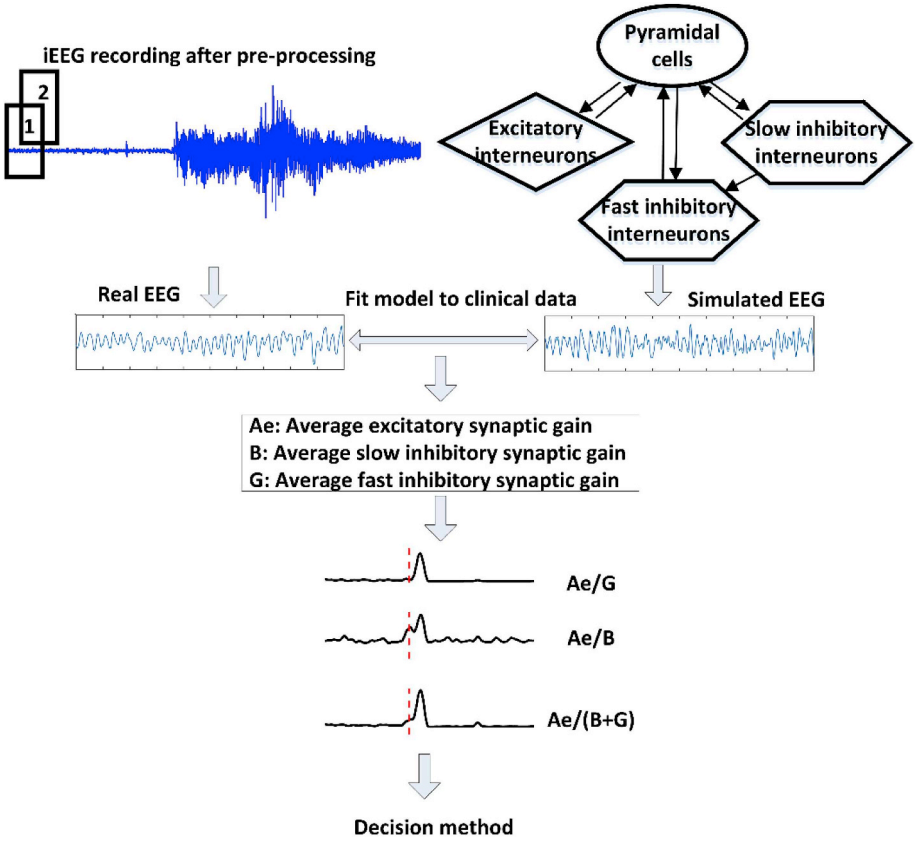

Fig. 1. Algorithm overview.

behavior. We assumed the cues did not change abruptly and a 30-s forward-reverse moving average filter was applied to smooth them. Similar strategies are often used in seizure detection algorithms [30–32], with a filter size from 30 s [30] to 5 min [31]. We have shown previously that varying the size of the moving average filter within a certain range had minor effect on the global trend of these cues [19]. As the recordings were processed with a sliding window, the decision was made for each successive window, with a resulting resolution corresponding to the step of the sliding window, i.e. 1s.

The threshold can be either fixed (i.e. keep constant for all patients) or adapted to each specific patient [18,33]. The patient-specific threshold was computed as being equal to k times the standard deviation (SD) above the mean of the background baseline (calculated from the first 5 min EEG of each recording), i.e. Eq. (1).

$$T_s = mean(C_b) + k * std(C_b) \quad (1)$$

Where T_s represents patient-specific threshold and k is a fixed parameter; C_b stands for the background baseline of any cue that is obtained from the first 5 min EEG of each recording. Since background EEG samples are centered on the mean, with some fluctuation expressed by their standard deviation, this threshold aims to determine when the samples cannot express background activity anymore because they evolve toward an epileptic seizure.

2.5. Performance analysis

Common performance metrics, namely sensitivity, false positive rate, mean false detection duration and detection delay [34], were used to evaluate the performance of the algorithm, which was obtained by comparing algorithm detection with manual scoring of the expert.

The *sensitivity* is defined as:

$$\text{sensitivity} = \frac{TP}{TP + FN}$$

where TP (True Positive) is the number of seizures identified by both algorithm and expert, and FN (False Negative) is the number of seizures identified by the expert but not by the algorithm. Since this study focused on early seizure detection, i.e. the detection of the onset of the seizure at an early stage, we chose to relate the definition of a TP to the seizure onset. A detection made within a time window between 5 s before seizure onset marked by the expert and 180 s after is considered as a TP. If no seizure is detected within this horizon, it is regarded as a FN. The choice of 5 s before seizure onset was justified and used in previous study [17]. A seizure lasts from a few seconds to a few minutes, mostly less than two or 3 min [35], sometimes longer than 5 [36] (> 2 min for most seizures in our database). We accounted for the duration of a seizure and chose 180 s after seizure onset as previously proposed [18].

The *False Positive Rate (FPR)* is defined as:

$$\text{FPR} = \frac{FP}{Total\ Time}$$

Where the *Total Time* denotes the total recording time in hours and FP (False Positive) is the number of seizures identified by the algorithm but not scored as a seizure by the expert. Considering the spiky nature of false detections [34,37], we joined all FPs lying very close (within 1 min) apart from each other, as previously proposed [34].

The *Mean False Detection Duration (MFDD)* is the average of the

durations of all false positives. It was reported as a complement of FPR and avoid possible misleading caused by the joint of subsequent and close false detections [34].

The *detection delay* is the time delay of a TP to the seizure onset marked by the expert.

Since the sensitivity of the algorithm can be increased by decreasing the threshold at the cost of higher FPR, and vice versa, Receiver Operator Characteristic (ROC) curves were computed to evaluate the algorithm globally for all threshold values. For patient-specific threshold, the value of the threshold varied by varying k in Eq. (1) and therefore is automatically adapted to each patient. In this study, the value of k was varied from 0 to 40. For fixed threshold, it varied identically for all patients. The algorithm performance was compared in terms of area under ROC curve (AUC), between patient-specific threshold and fixed threshold, as well as when different cues were used. We chose to express the ROC curve in terms of sensitivity against FPR (rather than sensitivity against specificity), as it is usually performed in seizure detection [14,17,38]. This choice allows to avoid the arbitrary choice of the length for non-seizure events (that is required for specificity) and to obtain balanced data (there are usually much more non-seizure events than seizures). Please note that, since the FPR can exceed one, the value of the AUC also can exceed one. A cut-off FPR of 5 was used for calculating the AUC.

Our database includes patients with various types of epilepsy, thus allows comparison of the performance of the algorithm among patient groups. After determining the cue that achieves the best performance, we further compared the algorithm performance on different patient groups, i.e. TLE, FLE and the others.

A leave-one-out cross-validation (LOO-CV) was performed to assess the performance of the system and determine the robustness of the estimated threshold. The performance reported with LOO-CV is almost an unbiased estimation of the performance of an algorithm would achieve on unseen data of infinite size once it is trained on all available data [34]. It was performed separately for each patient group, since the cues may differ intrinsically for each epilepsy type. For each patient group, all but one patients' data was collected for training the algorithm to determine the threshold, and the remaining patient's data for testing. The threshold was automatically determined such that the algorithm achieved the highest sensitivity in the training set while minimizing the FPR. We reported the value of the threshold for each patient and compared them among patient groups.

3. Results

3.1. Comparison among threshold strategies

Table 1 shows the AUCs obtained using different cues, i.e. Ae/G, Ae/B or Ae/(B + G), and the two threshold strategies, i.e. fixed threshold or patient-specific threshold, for the three patient groups separately and for all patients altogether. It can be seen that patient-specific and fixed thresholds allowed comparable AUC (Wilcoxon signed rank test: $p = 0.11$). Therefore, fixed threshold, considered more objective and stable since it does not depend on the choice of the window used to evaluate the background, was used in subsequent analysis. Results corresponding to LOO-CV with patient-specific threshold are given as supplementary materials (Table S1).

Table 1
Area under the ROC curve (AUC): comparison between fixed threshold and patient-specific threshold, and among the three cues for different patient groups separately and altogether.

	Ae/G		Ae/B		Ae/(B + G)	
	Fixed threshold	Patient-specific	Fixed threshold	Patient-specific	Fixed threshold	Patient-specific
TLE	4.36	4.37	3.55	3.55	4.60	4.58
FLE	2.89	2.94	2.88	2.93	3.05	3.15
Others	3.90	3.90	1.38	1.40	3.83	3.80
Altogether	3.91	3.91	3.18	3.19	4.05	4.11

3.2. Comparison among cues

The algorithm performance was compared in terms of AUC when individual cue was used. As shown in Table 1, the algorithm achieved the best performance (highest AUC) when Ae/(B + G) was used as the cue in TLE and FLE patients. For the “others” group (FTLE, PTOLE and OLE patients), the algorithm achieved comparable performance when Ae/(B + G) or Ae/G was used as a cue.

3.3. LOO-CV results

Individual results obtained from LOO-CV with Ae/(B + G) as a cue are given in Table 2. Overall, 74 out of 91 (81.32%) seizures were detected. The algorithm performance differed among patients. The sensitivity varied from 0% to 100% (74.13% ± 36.61%), the FPR ranged from 0 to 9.46 (median: 0.17, SD: 2.56) per hour and MFDD varied from 0s to 271.5 s (median: 18.7 s, SD: 70.5 s). Results are considerably better for TLE patients (sensitivity 93.33%, median FPR: 0.28 per hour, median MFDD: 19.1 s) than FLE patients (sensitivity: 60.87%, median FPR: 0.17 per hour, median MFDD: 9.3 s) and the 3 patients diagnosed with FTLE, POLE and OLE (sensitivity: 50%, median FPR: 0.17 per hour, median MFDD: 34.5 s). The average delay (between seizure onset annotated by the expert and automatic detection) was also calculated for each patient. It ranged from −217.0 s to 78.5 s (median: 1.75 s, SD: 64.5 s). Negative delay indicates the algorithm detected the seizure before the expert. The detection delay for TLE patients varied from −19.7 s to 80.0 s (median: 14.4 s, SD: 25.7 s). No seizures were detected in patients 7 and 8, diagnosed with FLE. For the remaining FLE patients, the average detection delay ranged from −217.0 s to 78.5 s (median: -3.25 s, SD: 102.0 s). Patients 12 and 13, diagnosed with FTLE and PTOLE respectively, showed a mean detection delay of 31.3 s and 28.0 s respectively. It was noted that patient 18, from the TLE group, showed a much higher FPR (9.46) compared to other TLE patients (0.65 ± 0.80). This patient was retrospectively analyzed by an expert neurologist (B.L.). Seizures were distinct. They resembled frontal lobe seizures although the seizures originated from temporal lobe. Also, some clinical manifestations were reproduced by fronto-orbital stimulations. Thus, it might be inappropriate to include this patient in the TLE group due to the potential existence of a pathological network between the temporal lobe and fronto-orbital region. We re-performed the LOO-CV procedure after removing this patient. The performance of the algorithm for other TLE patients did nearly not change. The median FPR for TLE group reduced to 0.16 per hour (SD: 0.80). We excluded patient 18 for the following analysis. Fig. 2 shows the ROC curves for the three patient groups obtained by varying the threshold values. As can be seen, the algorithm performed considerably better for TLE patients.

3.4. Analysis of threshold values

The boxplot of the thresholds determined by the LOO-CV procedure (Ae/(B + G) as a cue), for each patient group, is shown in Fig. 3. The values of the threshold did nearly not vary among TLE patients (0.1018 ± 6.9e-5). The values of the threshold varied more for FLE patients (0.1334 ± 0.0137) and had higher values compared to that of TLE patients (Mann-Whitney U test: $p < 0.001$). The values of the threshold for the other patients i.e. the ones diagnosed as PTOLE, FTLE and OLE (0.1007 ± 0.0055), on the other hand, were comparable to that of TLE patients (Mann-Whitney U test: $p = 0.5604$).

The values of threshold determined by LOO-CV are surprisingly consistent across TLE patients, suggesting a general excitation/

Table 2
iEEG data and leave-one-out cross-validation results for each patient. The total recording time, total number of seizures, total number of detected seizures, overall sensitivity, median false positive rate (FPR), median mean false detection duration (MFDD), median average detection delay and mean threshold for each patient group were provided separately (in bold). Patients 12, 13 and 14 were diagnosed with FTLE, PTOLE and OLE, respectively. TLE: Temporal Lobe Epilepsy; FLE: Frontal Lobe Epilepsy; FTLE: Fronto-Temporal Lobe Epilepsy; PTOLE: Parieto-Temporal-Occipital Lobe Epilepsy; OLE: Occipital Lobe Epilepsy; N/A: not applicable. The data in parentheses represents results after excluding patient 18 (see section 3.3).

Patient Group	Patient ID	Recording Time (hrs)	# of Seizures	Detected seizures	Sensitivity (%)	FPR (/hr)	MFDD (s)	Detection delay (s)	Threshold
TLE	1	35.38	10	10	100.00	2.06	25.9	1.3	0.1018
	3	38.12	9	9	100.00	0.00	0.0	−4.6	0.1018
	5	12.11	6	6	100.00	0.00	0.0	40.8	0.1018
	6	12.25	3	3	100.00	0.16	5.5	14.3	0.1018
	15	23.92	1	1	100.00	2.09	25.4	−3.0	0.1018
	17	21.15	5	4	80.00	1.47	22.3	33.0	0.1018
	18	10.25	3	3	100.00	9.46	36.0	−21.3	0.1018
	19	6.82	2	2	100.00	0.00	0.0	14.5	0.1018
	20	25.69	10	10	100.00	0.12	20.0	−0.2	0.1018
	21	9.95	5	3	60.00	0.40	23.8	18.3	0.1021
	22	16.77	2	1	50.00	0.00	0.0	78.0	0.1018
	23	24.67	4	4	100.00	0.89	18.2	38.8	0.1018
	Overall	**237.09 (226.84)**	**60 (57)**	**56 (53)**	**93.33 (92.98)**	**0.28 (0.16)**	**19.1 (18.2)**	**14.4 (14.5)**	**0.1018 (0.1018)**
FLE	2	15.78	4	1	25.00	0.00	0.0	9.0	0.1463
	4	21.74	5	2	40.00	0.00	0.0	78.5	0.1463
	7	5.69	1	0	0.00	0.00	0.0	N/A	0.1401
	8	17.80	2	0	0.00	0.00	0.0	N/A	0.1463
	9	14.17	3	3	100.00	7.62	271.5	−217.0	0.1181
	10	25.85	3	3	100.00	3.37	230.8	−115.7	0.1183
	11	8.76	3	3	100.00	0.34	18.7	52.3	0.1401
	16	5.74	2	2	100.00	5.40	120.4	−15.5	0.1121
	Overall	**115.53**	**23**	**14**	**60.87**	**0.17**	**9.3**	**−3.25**	**0.1334**
Others	12	16.16	3	3	100.00	0.06	3.0	31.3	0.1001
	13	6.33	2	1	50.00	2.85	40.0	28.0	0.0943
	14	11.72	3	0	0.00	0.17	34.5	N/A	0.1078
	Overall	**34.21**	**8**	**4**	**50.00**	**0.17**	**34.5**	**29.67**	**0.1007**

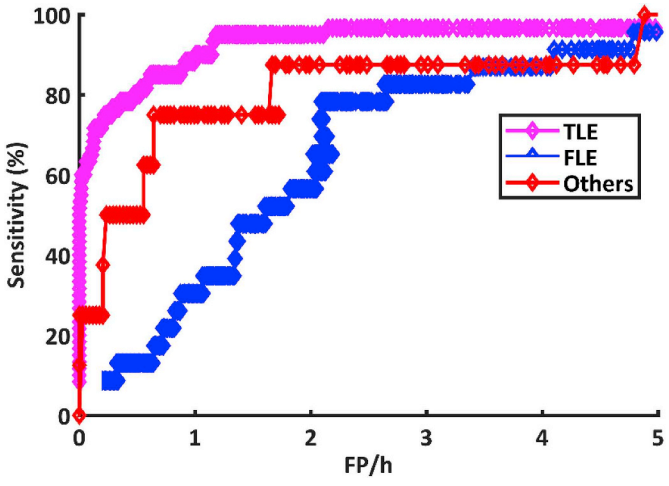

Fig. 2. ROC curves obtained for the three patient groups, i.e. TLE, FLE and others. TLE: temporal lobe epilepsy; FLE: frontal lobe epilepsy; FP/h: false positive per hour.

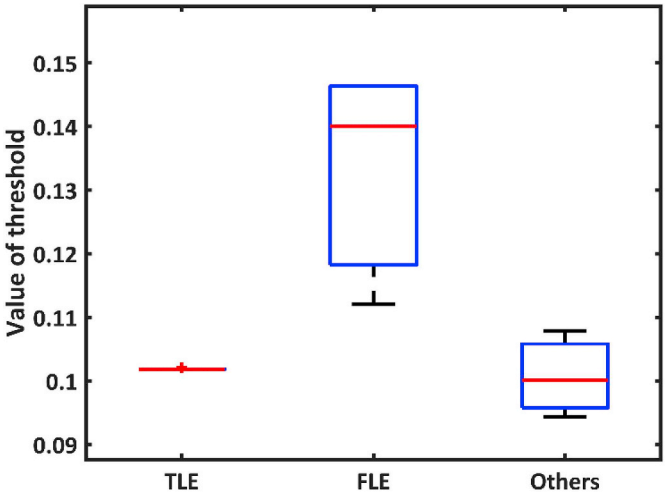

Fig. 3. The values of the threshold determined by the LOO-CV procedure, for each patient group, when Ae/(B + G) was used as the cue.

inhibition baseline during interictal period among them. To verity this, we analyzed the value of Ae/(B + G) during interictal periods for each TLE patient. The intra- and inter-patient variation in the value of Ae/(B + G) were evaluated as coefficient of variation (CV: the ratio of SD to the mean), expressed as a percentage. The intra-patient variation varied from 4.96% to 8.30% (mean ± SD: 6.80% ± 1.21%) and the inter-patient variation was 8.43%. Both intra- and inter-patient variation in the value of Ae/(B + G) were low (CV < 10%), showing that the Ae/(B + G) interictal baseline is rather constant, both for a given patient and across all patients. The histograms of Ae/(B + G) during interictal periods for all TLE patients are shown in Fig. 4 (the mean threshold for TLE patients shown in Fig. 3 is indicated by the vertical dash line). It can be seen that inter-patient variation is similar to intra-patient variation.

4. Discussion

We proposed a model-based approach to detect epileptic seizures at

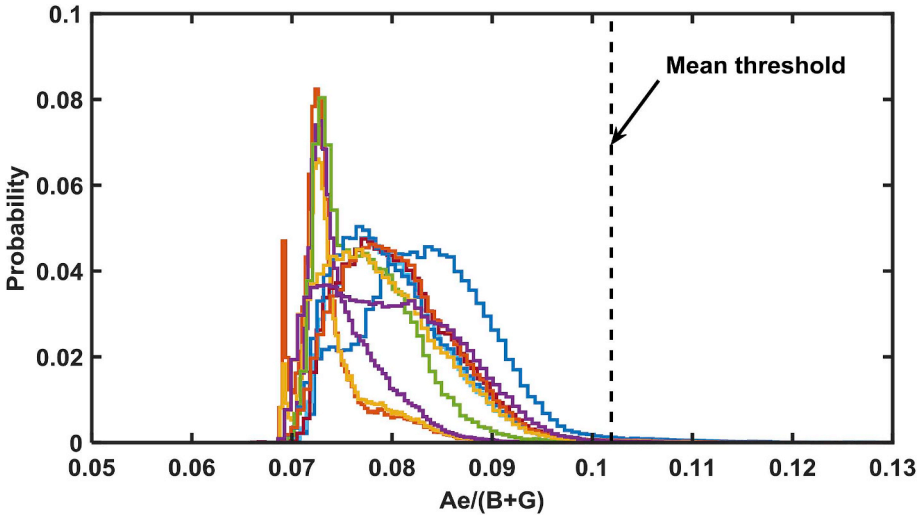

Fig. 4. The histogram of Ae/(B + G) during interictal periods for TLE patients. The vertical axis represents the probability of selecting an observation within that bin interval, and the sum over all the bins equals to 1. The vertical dash line indicates the mean thresholds for TLE patients.

an early stage based on the temporal evolution of average synaptic gains (excitatory Ae, slow and fast inhibitory B and G) identified from an NMM. Three cues, i.e. Ae/G, Ae/B and Ae/(B + G), all related to the balance between the excitation and inhibition, were used for seizure detection with a simple thresholding method. Results showed that Ae/(B + G) achieved best performance in terms of area under the ROC curve. The algorithm achieved comparable performance with patient-specific threshold, or with fixed threshold for all patients. It indicates that the inter-patient variations of the excitation/inhibition balance baseline are small. LOO-CV was conducted separately for three patient groups diagnosed with different types of epilepsy. Results were considerably better for TLE patients than FLE patients and others (FTLE, PTOLE and OLE patients): the sensitivity was 92.98%, the median FPR was 0.16 per hour with median MFDD of 18.2 s and the median detection delay was 14.5 s. This result is clinically interesting as TLE is the most common form of focal epilepsy. Of interest, the threshold determined by LOO-CV did nearly not vary among TLE patients, suggesting a general baseline of excitation/inhibition balance (at neuronal population level). This was further verified by analysis on the values of Ae/(B + G) during interictal periods for TLE patients, showing that the Ae/(B + G) interictal baseline is rather constant, both for a given patient and across all patients.

The dynamic balance between excitation and inhibition is a fundamental feature of normal brain activity at multiple scales, from individual neurons [39], ensembles [40] to networks [41]. In general, the balance of excitation and inhibition at neuronal level implies a constant ratio between excitatory to inhibitory inputs of a neuron and this balance is universal among pyramidal neurons and stabilized in time [39]. Our results suggested a general baseline of excitation/inhibition ratio during interictal periods among TLE patients and related seizure generation to the elevation of this ratio. A simple thresholding method on this ratio yielded therefore to good seizure detection results.

Both $GABA_{A,\ slow}$ and $GABA_{A,\ fast}$ inhibitory interneurons are involved in the generation of theta and gamma rhythms [42], which can often be observed in EEG seizure signals. It has also been shown in vitro that global optogenetic activation of mixed interneuron populations are more effective for seizure control, compared to targeting only one interneuron population, due to a more generalized GABA release [43]. Our results demonstrated that Ae/(B + G), i.e. excitation/(slow + fast inhibition), was more effective for seizure detection, than when only one inhibition was involved, i.e. Ae/G and Ae/B, and are therefore in line with these previous results.

In the first part of the study, fixed and patient-specific thresholds were compared. Results showed that fixed threshold achieved comparable AUC than patient-specific threshold. In the second part of the study, only fixed threshold was evaluated. This decision was made because fixed threshold was considered more objective and stable. Indeed, fixed threshold does not depend on the choice of the window used to evaluate the background. The patient-specific threshold, on the contrary, was set based on the first 5 min of EEG. If these first 5 min of EEG contains seizure activity, it could obviously affect the threshold, i.e. the threshold would be higher because it is based on cues that increase during seizure activity [19,20]. We could have carefully selected an EEG segment which is free of seizure activity to calculate the patient-specific threshold. But this would require prior selection of an EEG segment and, besides the time it requires, it also reduces the objectivity of the procedure.

The values of the threshold determined by LOO-CV were significantly different among different patient groups, suggesting distinct excitation/inhibition baseline among those groups, which, in turn, justified our cross-validation procedure by groups. However, whether this ratio during interictal periods could potentially give an indication about the type of epilepsy needs further investigation.

Among the 12 TLE patients in our database, 100% sensitivity was achieved for 9 of them. For the other 3 patients, 17, 21 and 22, 80% (4/5), 60% (3/5) and 50% (1/2) sensitivity was achieved. The 4 seizures that the algorithm failed to detect were subclinical seizures, which usually last for a very short duration (~10s in our case) and do not present any noticeable clinical signs or symptoms [44,45]. Therefore, the changes in cues might be smoothed out by the 30-s moving average filter used in our study. The cost of missing such seizures could possibly be of lower importance, depending on the application. In some seizure detection studies, subclinical seizures [14] and seizures with shorter duration [45] were even excluded from analysis. If we exclude these subclinical seizures from our analysis, our algorithm would have achieved 100% sensitivity for all TLE patients. We noted that patient 18 showed much higher FPR than other TLE patients. Seizures from this patient had distinct features. Some clinical manifestations were reproduced by fronto-orbital stimulations and the seizures resembled frontal lobe seizures, although they originated from temporal lobe. Thus, there might be a pathological network between temporal lobe and fronto-orbital region for this patient that is distinct from all other TLE patients. Hence, it might be inappropriate to include him/her in the TLE group. Excluding this patient from the LOO-CV procedure had minor effect on algorithm performance for other TLE patients.

The algorithm's better performance with TLE patients was expected

Table 3
Comparison of the performance of our algorithm for TLE group with previously published algorithms, in terms of sensitivity, false positive rate (FPR) and detection delay.

Authors	# of patients	Data length (h)	# of seizures	Sensitivity (%)	FPR (/h)	Detection delay (s)
Kharbouch A et al. [51]	10	875	67	97.00	0.03	5.00
Aarabi et al. [14]	21	302.7	78	98.70	0.27	11.00
Zhang et al. [44]	21	539	59	92.06	0.34	1.2
Rabbi et al. [38]	20	112.45	56	95.80	0.26	15.80
Geng et al. [52]	20	255	55	96.67	0.27	–
Bandarabadi et al. [53]	11	1785	183	86.90	0.06	13.10
Edakawa et al. [49]	7	1546	21	92.90	0.02	–
Zhang et al. [45]	17	463	51	92.00	0.17	12.00
Donos et al. [17]	10	10	125	93.84	0.07	1.75
Grewal et al. [54]	19	389	100	89.4	0.22	17.1
Hocepied et al. [18]	5	28.58	30	96.00	0.14	14.34
Average	15	573.25	75	93.75	0.17	10.14
This paper	11	226.84	57	92.98	0.16	14.5

for two reasons. First, the NMM has been reported to be capable of simulating seizures similar to the ones recorded from TLE patients [21]. Second, the implicit assumption underlying the model-based seizure detection approach is that the dynamics of ictogenesis can be captured by smooth variations of several system parameters, which was true in TLE, but not in FLE [46]. It was proposed that TLE seizures were caused by a deformation of the attractor leading to a gradual evolution onto the ictal state, thus seizures can be detected by analyzing the gradual change in dynamics [18]. This contrast with FLE seizures that were reported to be caused by a perturbation in a bistable state without change in parameters [47] and therefore might be rather difficult to detect [46]. Regarding the third group (i.e. with FTLE, PTOLE and OLE), individual results were also obtained by LOO-CV, even though they were diagnosed with different types of epilepsy. More robust and better results might be achieved, provided an appropriate model that describes EEG dynamics of these specific types of epilepsy.

Direct comparison of results with other published seizure detection algorithms is difficult due to the heterogeneity of datasets and metrics to assess performance [34,48]. However, we attempted to compare our method with other algorithms tested on continuous human iEEG recordings of TLE patients that also reported their results in terms of sensitivity, FPR and detection delay (see Table 3). It can be seen that our algorithm achieved comparable sensitivity and FPR, with a slightly higher detection delay (4.36 s higher on average).

Besides the divergence in datasets, the testing and performance evaluation strategy also differ. For example, Aarabi et al. trained their model on 40% of all iEEG data and tested it on all data rather than on the rest of it [14], which might overestimate the performance since the training data was also used for testing. Edakawa et al. excluded 30 min before and after the seizure from the analysis [49], which might decrease the FPs caused by the spikes before seizures. Aarabi et al. excluded subclinical seizures from their analysis [14] and Zheng et al. rejected patients with shorter seizures [45]. In this regard, the comparison might have been disadvantageous for our algorithm.

Focusing on the detection delay, in Ref. [18], a larger detection horizon was used, i.e. from 3.5 min before seizure onset to 3.5 min after. Furthermore, in Ref. [44], the authors used a collar technique where each detected seizure event was extended several epochs on both sides. Both approaches might have affected the latency of seizure detection and resulted in a shorter detection delay. Therefore, such comparison might have been disadvantageous for our algorithm. Furthermore, the clinical impairment of a patient could happen up to 30 s after the electrographic onset of a seizure, even with the most rigorous definitions [50]. Thus, the detection delay provided by our algorithm could be acceptable for most patients. It could also be improved at a cost of higher FPR.

The aim of our work rather lies in relating ictogenesis with physiological parameters change and arguing in favor of the feasibility of such a model-based approach than proposing a detector that outperforms the others. One distinct advantage of our methodology is that it offers insights into epileptic seizure occurrence by linking the mathematics of nonlinear systems and neurophysiology. In turn, any advance in better understanding of seizure generation, can be directly translated to this algorithm to enhance seizure detection. The dynamic balance between excitation and inhibition is essential for neural homeostasis and normal function of the brain, and its breakdown could give rise to epileptic seizures [55]. Our methodology allows to track the gradual change of average excitatory, slow and fast inhibitory synaptic gains from the iEEG recording and relates seizure generation with the elevation of excitation/inhibition ratio. This can be interpreted as a path to an epileptic state space of the model.

The variability of EEG waveforms across, even within, patients, which makes training of most conventional classifier difficult, does not affect the choice of the threshold for TLE patients. The threshold determined by LOO-CV is nearly constant for all TLE patients tested, which permits direct use of our algorithm on unseen data without training. Specific needs (higher sensitivity, lower false positive rate or earlier detection) can then, if needed, be achieved easily by fine-tuning the threshold. This greatly reduces the cost for training a detector, which normally requires both massive data and time. Being surprisingly simple, our algorithm achieved competitive performance and could be improved in terms of false positive rate by including a post-processing procedure [14,45].

To the best of our knowledge, only three model-based seizure detection or prediction algorithms have been previously proposed.

A model-based seizure detection algorithm has been previously proposed by Roessgen et al. for the newborns [56]. The authors included a seizure-generating component in the NMM as a driver to seizure activities, to describe any physiological mechanisms for generating seizures. The EEG spectrum was divided into two separate components, one corresponds to the background EEG, the other to the seizure EEG, which can be estimated from EEG data. The ratio of these two components was employed as a cue for detecting seizures. The model they used therefore assumed an outside epileptogenic driver to account for the general effect of various mechanisms, thus no hint about seizure generation can be derived. In our work, we directly relate the parameter of a physiologically based model to neurological mechanisms. Our algorithm relies on better understanding of ictogenesis by relating the occurrence of a seizure to the ratio between average synaptic gains of the excitatory and inhibitory neuronal population, i.e. excitation/inhibition balance, which was proposed to be one of the possible mechanisms of ictogenesis [40,57,58].

A model-based approach has already been proposed for hippocampal and or neocortical seizure prediction [33]. Six contacts were

selected for each patient, out of which three were inside the epileptogenic zone whereas three were from remote regions. For each of the six contacts, twelve model parameters were estimated by fitting the NMM to the power spectral and seizures were predicted by investigating changes in parameters prior to seizures. For each patient, six contacts were manually chosen. Out of them, the contacts and thresholds used for seizure prediction (up to 72 thresholds, since there is 6 contacts and 12 parameters per contact) as well as their values were optimized during the training process. The method is therefore quite complex, the established patient-specific rules were difficult to interpret and were rather behavioral than relying on physiological assumptions [33]. Our method, on the contrary, detects seizures upon the elevation of excitation/inhibition ratio, which corresponds to physiological advances and has a straightforward interpretation. Of note, segments highly contaminated by spikes had to be rejected to reduce their effect on the total spectral power of the iEEG segments. Our algorithm is more tolerant to these activities.

Our group also previously proposed a model-based seizure detection algorithm [18]. However, it used a simpler model that did not allow simulation of more subtle neural behavior. It did not either benefit from the analysis of ictogenesis mentioned above [40,57,58]. This notably led to major two differences, in the seizure detection algorithm and in the parameter identification procedure. In our previous work, the procedure used could not propose a cue on which the seizure detection algorithm could be based that specifically reflects the occurrence of a seizure. The detection algorithm therefore also had to be able to face the variation of the cue due to the other features present in the EEG. Spikes, for instance, affected the cue more than seizures. In the present work, the seizure detection algorithm is a simple thresholding method. In our previous work, the parameter identification procedure included a spike detection algorithm [59,60] to specifically focus on spikes. The algorithm therefore had an a priori information on the presence of spikes and some bias might therefore have been introduced. In the present work, the model and method used do not include any a priori information about any specific EEG feature. Also, the length of the dataset is much larger in the present work.

We used simple thresholding method to detect seizures. More complex decision algorithms, such as a statistical model or learning methods (e.g. neural networks) could provide better results. However, the interpretability of algorithm behavior could then be reduced. Neural networks have been implemented in a trial study. We only tried a simple network structure, with one input layer, one hidden layer and one output layer. The input layer has three input neurons (corresponding to three cues, Ae/G, Ae/B and Ae/(B + G)). The hidden layer has 10 neurons and the output layer has 2 neurons (corresponding to the 2 classes, seizure and non-seizure). Even with such a small feed-forward network, 62 parameters needed to be trained and the behavior of the network was not as straightforward as simple thresholding. This could somewhat counterbalance the transparent approach of using a physiological model-based approach. Leave-one-out cross-validation results showed that the simple neural network did not improve the seizure detection algorithm much (see the supplementary materials Tables S2 and S3) and even sometimes showed results that were slightly worse. In this paper, we chose to focus on a thresholding method mainly because the behavior of the algorithm can be directly related to neurophysiology, i.e. the elevation of the ratio of excitation and inhibition indicates the occurrence of a seizure.

The proposed method presents various benefits. Most importantly, it is physiologically interpretable and extendable. It could provide insights into seizure genesis, and in turn, further scientific advances can be translated into this method to enhance seizure detection. Besides, it is simple, straightforward, effective, and it shows positive results on TLE patients. One limitation of the study is that the algorithm required a prior knowledge from an expert, as one derivation, corresponding to the earliest involved electrode, was pre-selected. This may be considered as a drawback of this method. However, routine clinical evaluations of epileptic patients that undergo iEEG typically already include an estimation of such a derivation. Furthermore, it is very common, even important to select the proper channels for each individual in seizure detection applications [17,33], in order to achieve satisfactory performance. Another limitation is that the proposed algorithm has only been validated on iEEG. The proposed methodology could be translated to scalp EEG to be used in other clinical fields (i.e. routine scalp EEG).

The proposed method could be useful for clinical purpose. First, the method could serve as a clinical tool that could help the clinical staff to locate the seizure events among massive EEG data easily and provide information about the type, location, and frequency of seizure events. Since the tool methodology follows a model-based approach, it is transparent and understandable, and advances in our understanding of seizure genesis could be included to enhance seizure detection. Second, the model used for the algorithm could also give straightforward understanding of the mechanism governing epileptic seizure genesis for a given patient, as previously reported [19,20]. Better understanding of seizure events promotes better decision regarding treatment strategy. Therefore, the present method has its potential use in diagnosis of epilepsy.

In conclusion, we have described an algorithm that relies on parameter identification of a physiological-based model to detect seizures. We have shown that the seizures can be detected based on the temporal evolution of physiologically meaningful parameters and the seizure occurrence can be related to the elevation of the excitation/inhibition ratio. Of interest, the threshold determined by LOO-CV was surprisingly constant among TLE patients, suggesting a general baseline of excitation/inhibition balance underlying background iEEG and the algorithm could be used directly on unseen data without training. There are several possibilities for future directions of the presented work. First, a logical step is to validate this methodology for scalp EEG as it is non-invasive and easily accessible. Second, a more complex model that describes more subtle neuronal behavior could be implemented, for instance, network of NMMs. Such models consider the spatiotemporal dynamics of EEG at a larger spatial scale and allow inclusion of multiple contacts, and thus might provide more reliable seizure detection. Third, the proposed method works best on TLE patients since the specific model simulated best dynamics underlying temporal lobe seizures. Future effort could be devoted to improving algorithm performance for other types of epilepsy, i.e. by adapting the model for better simulating EEG dynamics of other types of epilepsy. At last, the possible physiological reasons underlying both false negatives and false positives could be further investigated. The undetected seizures might involve different mechanisms that worth studying. Similarly, the false positives could indicate physiological changes during interictal period, which could be of great scientific interest. Such investigation could provide a more rational classification of epileptic seizures and provide new insights into multiple mechanisms underlying both interictal and ictal activities.

Contributors

Xiaoya FAN designed the study, analyzed and interpreted the data and wrote the manuscript. The other coauthors made a critical revision of the manuscript. Nicolas GASPARD acquired and annotated the data, gave his medical expertise on interpretation and analysis of data. Benjamin LEGROS acquired and annotated the data, gave his medical expertise on interpretation and analysis of data. Federico LUCCHETTI provided advice on data analysis. Rudy ERCEK provided advice on data analysis. Antoine NONCLERCQ designed and supervised the study.

Conflict of interest statement

None Declared.

Acknowledgement

This work was supported by the China Scholarship Council (CSC) and Fonds David et Alice Van Buuren & Fondation Jaumotte-Demoulin.

Appendix A. Supplementary data

Supplementary data to this article can be found online at https://doi.org/10.1016/j.compbiomed.2019.02.005.

References

[1] A.K. Ngugi, et al., Estimation of the burden of active and life-time epilepsy: a meta-analytic approach, Epilepsia 51 (5) (2010) 883–890.
[2] R.S. Fisher, et al., Epileptic seizures and epilepsy: definitions proposed by the international league against epilepsy (ILAE) and the international bureau for epilepsy (IBE), Epilepsia 46 (4) (2005) 470–472.
[3] S.B. Wilson, et al., Seizure detection: correlation of human experts, Clin. Neurophysiol. 114 (11) (2003) 2156–2164.
[4] J. Engel, Approaches to refractory epilepsy, Ann. Indian Acad. Neurol. 17 (Suppl 1) (2014) S12–S17.
[5] R.S. Fisher, et al., The impact of epilepsy from the patient's perspective I. Descriptions and subjective perceptions, Epilepsy Res. 41 (1) (2000) 39–51.
[6] R.S. Fisher, A.L. Velasco, Electrical brain stimulation for epilepsy, Nat. Rev. Neurol. 10 (5) (2014) 261–270.
[7] M.J. Morrell, Responsive cortical stimulation for the treatment of medically intractable partial epilepsy, Neurology 77 (13) (2011) 1295–1304.
[8] S.N. Baldassano, et al., Crowdsourcing seizure detection: algorithm development and validation on human implanted device recordings, Brain 140 (6) (2017) 1680–1691.
[9] A. Garces Correa, et al., Automatic detection of epileptic seizures in long-term EEG records, Comput. Biol. Med. 57 (2015) 66–73.
[10] Y.U. Khan, J. Gotman, Wavelet based automatic seizure detection in intracerebral electroencephalogram, Clin. Neurophysiol. 114 (5) (2003) 898–908.
[11] Y. Kumar, M.L. Dewal, R.S. Anand, Epileptic seizures detection in EEG using DWT-based ApEn and artificial neural network, Signal Image Video P 8 (7) (2014) 1323–1334.
[12] K. Fu, et al., Classification of seizure based on the time-frequency image of EEG signals using HHT and SVM, Biomed. Signal Proces 13 (2014) 15–22.
[13] M.Z. Parvez, M. Paul, Epileptic seizure detection by analyzing EEG signals using different transformation techniques, Neurocomputing 145 (2014) 190–200.
[14] A. Aarabi, R. Fazel-Rezai, Y. Aghakhani, A fuzzy rule-based system for epileptic seizure detection in intracranial EEG, Clin. Neurophysiol. 120 (9) (2009) 1648–1657.
[15] A. Subasi, Application of adaptive neuro-fuzzy inference system for epileptic seizure detection using wavelet feature extraction, Comput. Biol. Med. 37 (2) (2007) 227–244.
[16] M. Mursalin, et al., Automated epileptic seizure detection using improved correlation-based feature selection with random forest classifier, Neurocomputing 241 (2017) 204–214.
[17] C. Donos, M. Dumpelmann, A. Schulze-Bonhage, Early seizure detection algorithm based on intracranial EEG and random forest classification, Int. J. Neural Syst. 25 (5) (2015) 1550023.
[18] G. Hocepied, et al., Early detection of epileptic seizures based on parameter identification of neural mass model, Comput. Biol. Med. 43 (11) (2013) 1773–1782.
[19] X. Fan, et al., Dynamics underlying interictal to ictal transition in temporal lobe epilepsy: insights from a neural mass model, Eur. J. Neurosci. 47 (3) (2018) 258–268.
[20] X. Fan, et al., Seizure evolution can be characterized as path through synaptic gain space of a neural mass model, Eur. J. Neurosci. 48 (9) (2018) 3097–3112.
[21] F. Wendling, et al., Epileptic fast activity can be explained by a model of impaired GABAergic dendritic inhibition, Eur. J. Neurosci. 15 (9) (2002) 1499–1508.
[22] F. Wendling, et al., Interictal to ictal transition in human temporal lobe epilepsy: insights from a computational model of intracerebral EEG, J. Clin. Neurophysiol. 22 (5) (2005) 343–356.
[23] A. Lopez-Cuevas, et al., State and parameter estimation of a neural mass model from electrophysiological signals during the status epilepticus, Neuroimage 113 (2015) 374–386.
[24] T. Kameneva, et al., Neural mass models as a tool to investigate neural dynamics during seizures, J. Comput. Neurosci. 42 (2) (2017) 203–215.
[25] J. Ashburner, SPM: a history, Neuroimage. 62 (2) (2012) 791–800.
[26] K.J. Friston, L. Harrison, W. Penny, Dynamic causal modelling, Neuroimage 19 (4) (2003) 1273–1302.
[27] R.N. Henson, et al., A parametric empirical bayesian framework for the EEG/MEGinverse problem: generative models for multi-subject and multi-modal integration, Front. Hum. Neurosci. 5 (2011).
[28] F. Wendling, et al., Relevance of nonlinear lumped-parameter models in the analysis of depth-EEG epileptic signals, Biol. Cybern. 83 (4) (2000) 367–378.
[29] J. Engel Jr., C. Wilson, A. Bragin, Advances in understanding the process of epileptogenesis based on patient material: what can the patient tell us? Epilepsia 44 (Suppl 12) (2003) 60–71.
[30] S. Li, et al., Seizure prediction using spike rate of intracranial EEG, IEEE Trans. Neural Syst. Rehabil. Eng. 21 (6) (2013) 880–886.
[31] K. Gadhoumi, et al., Seizure prediction for therapeutic devices: a review, J. Neurosci. Methods 260 (2016) 270–282.
[32] A. Bhattacharyya, R.B. Pachori, A multivariate approach for patient-specific EEG seizure detection using empirical wavelet transform, IEEE Trans. Biomed. Eng. 64 (9) (2017) 2003–2015.
[33] A. Aarabi, B. He, Seizure prediction in hippocampal and neocortical epilepsy using a model-based approach, Clin. Neurophysiol. 125 (5) (2014) 930–940.
[34] A. Temko, et al., Performance assessment for EEG-based neonatal seizure detectors, Clin. Neurophysiol. 122 (3) (2011) 474–482.
[35] W.H. Theodore, et al., The secondarily generalized tonic-clonic seizure: a videotape analysis, Neurology 44 (8) (1994) 1403–1407.
[36] E. Trinka, J. Hofler, A. Zerbs, Causes of status epilepticus, Epilepsia 53 (Suppl 4) (2012) 127–138.
[37] A.B. Gardner, et al., One-class novelty detection for seizure analysis from intracranial EEG, J. Mach. Learn. Res. 7 (2006) 1025–1044.
[38] A.F. Rabbi, R. Fazel-Rezai, A fuzzy logic system for seizure onset detection in intracranial EEG, Comput. Intell. Neurosci. 2012 (2012).
[39] M. Xue, B.V. Atallah, M. Scanziani, Equalizing excitation-inhibition ratios across visual cortical neurons, Nature 511 (7511) (2014) 596–600.
[40] N. Dehghani, et al., Dynamic balance of excitation and inhibition in human and monkey neocortex, Sci. Rep. 6 (2016) 23176.
[41] A. Bhatia, S. Moza, U.S. Bhalla, Precise Excitation-Inhibition Balance Controls Gain and Timing in hippocampus, bioRxiv, 2017.
[42] J.A. White, et al., Networks of interneurons with fast and slow gamma-aminobutyric acid type A (GABAA) kinetics provide substrate for mixed gamma-theta rhythm, Proc. Natl. Acad. Sci. U. S. A. 97 (14) (2000) 8128–8133.
[43] M. Ledri, et al., Global optogenetic activation of inhibitory interneurons during epileptiform activity, J. Neurosci. 34 (9) (2014) 3364–3377.
[44] Y. Zhang, W. Zhou, S. Yuan, Multifractal analysis and relevance vector machine-based automatic seizure detection inintracranial EEG, Int. J. Neural Syst. 25 (6) (2015) 1550020.
[45] Y.X. Zheng, et al., An automatic patient-specific seizure onset detection method using intracranial electroencephalography, Neuromodulation 18 (2) (2014) 79–84.
[46] F. Lopes da Silva, et al., Epilepsies as dynamical diseases of brain systems: basic models of the transition between normal and epileptic activity, Epilepsia 44 (Suppl 12) (2003) 72–83.
[47] G. Baier, et al., The importance of modeling epileptic seizure dynamics as spatio-temporal patterns, Front. Physiol. 3 (2012).
[48] S.B. Wilson, R. Emerson, Spike detection: a review and comparison of algorithms, Clin. Neurophysiol. 113 (12) (2002) 1873–1881.
[49] K. Edakawa, et al., Detection ofepileptic seizures using phase–amplitude coupling in intracranial electroencephalography, Sci. Rep. 6 (2016) 25422.
[50] C.C. Jouny, P.J. Franaszczuk, G.K. Bergey, Improving early seizure detection, Epilepsy Behav. 22 (2011) S44–S48.
[51] A. Kharbouch, et al., An algorithm for seizure onset detection using intracranial EEG, Epilepsy Behav. 22 (Suppl 1) (2011) S29–S35.
[52] D. Geng, et al., Epileptic seizure detection based on improved wavelet neural networks in long-term intracranial EEG, Biocybern. Biomed. Eng. 36 (2) (2016) 375–384.
[53] M. Bandarabadi, et al., Early seizure detection using neuronal potential similarity: a generalized low-complexity and robust measure, Int. J. Neural Syst. 25 (5) (2015) 1550019.
[54] S. Grewal, J. Gotman, An automatic warning system for epileptic seizures recorded on intracerebral EEGs, Clin. Neurophysiol. 116 (10) (2005) 2460–2472.
[55] J. Ziburkus, J.R. Cressman, S.J. Schiff, Seizures as imbalanced up states: excitatory and inhibitory conductances during seizure-like events, J. Neurophysiol. 109 (5) (2013) 1296–1306.
[56] M. Roessgen, A.M. Zoubir, B. Boashash, Seizure detection of newborn EEG using a model-based approach, IEEE Trans. Biomed. Eng. 45 (6) (1998) 673–685.
[57] T. Blauwblomme, P. Jiruska, G. Huberfeld, Mechanisms of ictogenesis, Int. Rev. Neurobiol. 114 (2014) 155–185.
[58] J. Engel Jr., Excitation and inhibition in epilepsy, Can. J. Neurol. Sci. 23 (3) (1996) 167–174.
[59] A. Nonclercq, et al., Spike detection algorithm automatically adapted to individual patients applied to spike and wave percentage quantification, Neurophysiol. Clin. 39 (2) (2009) 123–131.
[60] A. Nonclercq, et al., Cluster-based spike detection algorithm adapts to interpatient and intrapatient variation in spike morphology, J. Neurosci. Methods 210 (2) (2012) 259–265.